Analyst

Accepted Manuscript

ROYAL SOCIETY OF CHEMISTRY

www.rsc.org/analyst

Analyst

A single-molecule digital enzyme assay using alkaline phosphatase with a cumarin-based fluorogenic substrate

Yusuke Obayashi[1], Ryota Iino[2,3], Hiroyuki Noji[1,4]*

[1]Department of Applied Chemistry, The University of Tokyo, Japan

[2]Okazaki Institute for Integrative Bioscience, Institute of Molecular Science, National Institutes of Natural Sciences, Japan

[3]SOKENDAI (The Graduate University for Advanced Studies)

[4]CREST, Japan Science and Technology Agency

*Corresponding author:

Tel: +81 3 5841 7252, Fax: +81 3 5841 1872, E-mail: hnoji@appchem.t.u-tokyo.ac.jp

Abstract

Digitalization of fluorogenic enzymatic assays through the use of femtoliter chamber array technology is an emerging approach to realizing highly quantitative bioassays with single-molecule sensitivity. However, only a few digital fluorogenic enzyme assays have been reported, and the variations of the digital enzyme assay are basically limited to fluorescein- and resorufin-based fluorogenic assays. This limitation hampers realization of multiplex digital enzyme assay such as digital enzyme-linked immunosorbent assay (ELISA). In this study, after optimization of buffer condition, we achieved single-molecule digital enzyme assay of alkaline phosphatase (ALP) with a cumarin-based fluorogenic substrate, 4-methylunbelliferyl phosphate (4-MUP). When ALP molecules were encapsulated in 44-femtoliters chamber array at low ratio less than 1 molecules per chamber, each chamber showed discrete fluorescence signal in an all-or-none manner, allowing the digital counting of the number of active enzyme molecules. The fraction of fluorescent chambers linearly decreased with the enzyme concentration, obeying the Poisson distribution as expected. We also demonstrated dual-color digital enzyme assay of ALP/4-MUP and β-galactosidase (β-gal)/resorufin-β-D-galactopyranoside combination. The activities of single ALP and β-gal molecules were clearly detected simultaneously. The method developed in this study will enable us to carry out parallelized, multiplex digital ELISA.

Introduction

Miniaturization of bioassay systems provides many benefits to bioanalysis, such as massive parallelization, reductions in sample volumes, and more rapid responses due to the large surface-to-volume ratio.[1,2] Another important benefit of the downsizing of reaction volumes is higher sensitivity. A particular case is single-molecule fluorogenic enzyme assay using femtoliter chambers (hereafter referred to as the digital enzyme assay),[3-6] individual enzyme molecules are stochastically encapsulated with fluorogenic assay mixture in femtoliter-sized reactor chambers, and the catalytic activity is detected as the fluorescent signal from reaction product molecules accumulated in the femtoliter chambers. The mean turnover rate of enzymes is around 10 turnovers/s.[7] In a cube of 1 μm, which corresponds to 1 femtoliter, the concentration of reaction products reaches the micromolar range in a few minutes, allowing it to be readily detectable with a conventional fluorescent microscope.

In a pioneering study of a single-molecule enzyme assay in femtoliter-scaled reactors,[8] a diluted solution of β-galactosidase (β-gal) was partitioned in 7–30 μm water-in-oil (W/O) droplets with a fluorescein-based fluorogenic substrate at less than 1 enzyme molecule per droplet. The fluorescence signals from the droplets exhibited an all-or-none manner; while most droplets were not fluorescent, some showed clear fluorescence. The fraction of fluorescent droplets exhibited good linearity with the enzyme concentration, indicating that partitioning of the fluorogenic assay mixture into femtoliter reactors enabled detection of the catalytic activity of a single β-gal molecule. However, due to the inherent large heterogeneity of the W/O droplets prepared in this technique (which was developed over 50 years ago), this approach did not become widespread as an analytical method until microfabrication technology allowed generation of the femtoliter chambers with identical shapes and volumes. In 2005, Rondelez et al. first reported the digital counting of active enzyme molecules through the use of a microfabricated chamber system.[6] They prepared a microfabricated PDMS sheet with identically shaped micron-sized wells on the surface and encapsulated enzyme solution between the fabricated PDMS sheet and glass coverslip by mechanically pressing the PDMS sheet against a glass coverslip. When the enzyme solution was diluted to a ratio of less than 1 enzyme molecule per chamber, individual chambers showed discrete fluorescence signals in the all-or-none fashion; while the most of chambers remained non-fluorescent, few chambers showed fluorescence, and only a few showed fluorescence signals with double intensity, indicating the encapsulation of zero, one, or two molecules in each chamber, respectively. This work demonstrated that a very simple microdevice allows the formation of identically shaped femtoliter chambers and enables the single-molecule detection of enzyme molecules and

quantification of enzyme concentrations by directly counting the number of enzyme molecules (i.e., digital counting).

In recent years, several different formats for the femtoliter chamber system have been reported. For example, researchers reported a femtoliter chamber array system formed from a plain PDMS sheet and a chemically etched optical fiber bundle.[9] Additionally, Sakakihara et al. developed an array system of W/O droplets that formed on micron-sized hydrophobic patterns on glass.[10] Moreover, Ge et al. integrated a droplet chamber system in a microfluidic flow channel to form a gradient of the trapping probability of target molecules along the microchannel.[3] This system enables the automatic preparation of dilution series of specimen, allowing digital counting of enzyme molecules in a wide dynamic range. A microfluidic system for the generation and analysis of freestanding femtoliter droplets was also used for digital counting of enzyme molecules.[11] Recently, an arrayed lipid bilayer chamber system (ALBiC) was developed that allows digital counting and analysis of active transporter membrane proteins.[12]

Recently, application of femtoliter chamber arrays is also expanding. For example, PDMS-based femtoliter chamber arrays have been used for measurement of the chemomechanical coupling efficiency of a single rotary molecular motor protein[13] and for detection of individual translation events in single bacterial cells.[14] Many reports have described other applications of femtoliter chamber array systems that provide high sensitivity and/or high-throughput capacity, including DNA sequencing,[15] single-cell drug efflux activity analysis,[16] *in vitro* translation,[17] and single-enzyme analysis.[4,18] Among them, one of the most important applications is the digital enzyme-linked immunosorbent assay (ELISA),[3,11,19,20] in which antigen molecules recognized by enzyme-conjugated antibodies are individually entrapped in a chamber, and the number of antigen molecules is counted as the number of femtoliter chambers showing enzymatically produced fluorescence signal. Although the first report of a digital ELISA used the PDMS-etched optical fiber plate system,[20] droplet-based array systems have been frequently used in recent studies.[3,19,21] The digital ELISA has largely improved the limit of detection (LOD) down to the femto- or attomolar range, realizing the ultrasensitivity of diagnostic ELISAs.

Compared with the active development of platforms and expansion of applications of femtoliter chamber-based digital bioassays, variety of fluorogenic enzyme assays is still limited; however, researchers are hoping to develop parallelized digital counting assays, such as multiplex digital ELISAs, for improved analysis of multiple targets. To date, the chemistry of fluorogenic assays has mainly been based on three major fluorescent dyes: fluorescein, resorufin, and cumarin. Due to its high photostability and high fluorescent intensity, fluorescein is the first choice of probes; the first

digital enzyme assay used a fluorescein derivative conjugated with galactose.[6] Subsequently, digital enzyme assays with resorufin-based fluorogenic substrates were conducted for detection of β-gal,[22] β-glucuronidase,[4] and horseradish peroxidase.[18] Although resorufin and fluorescein fluorescence signals are spectrally separable, the excitation and emission spectra overlap, causing fluorescence cross-talk. Therefore, simultaneous, dual-color digital enzyme assays using fluorescein- and resorufin-based fluorogenic assays have not been attempted. Since cumarin-based fluorogenic assays use excitation and emission wavelengths much shorter than those of fluorescein and resorufin, it will be suitable for dual digital enzyme assays with these dyes. However, digital enzyme assays using cumarin-based fluorogenic substrates have not been reported. In this study, we developed a digital enzyme assay with a cumarin-based fluorogenic substrate for detection of *Escherichia coli* alkaline phosphatase (ALP), which is widely used in diagnostic ELISA.

Results

Before testing the digital enzyme assay with a cumarin-based fluorogenic substrate, we explored the optimal buffer conditions for catalytic reaction of ALP in solution. To obtain a high fluorescent signal, we used a mutant ALP (D101S) from *E. coli*, for which the V_{max} was 35-fold higher than that for the wild-type.[23] We used 4-methylunbelliferyl phosphate (4-MUP) as the fluorogenic substrate for ALP; 4-MUP is a phosphorylated cumarin derivative and hydrolyzed into inorganic phosphate and 4-metylunbelliferon (4-MU) (Fig. 1). While 4-MUP is non-fluorescent, 4-MU emits fluorescence (excitation peak: 372 nm, emission peak: 445 nm). The enzymatic activity of ALP was monitored by determining the fluorescence of 4-MU. Figure 2A shows typical time courses of the fluorogenic assay at different initial concentrations of 4-MUP. The concentrations of 4-MU increased linearly for 300 s, indicating constant turnover rates at this time scale under the condition used. Furthermore, the slope of the time course increased as 4-MUP concentration increased, indicating increased activity of ALP.

Next, we examined the effects of diethanolamine (DEA), which enhances the transphosphorylation activity of ALP as an acceptor of inorganic phosphate.[24] We also tested the effects of magnesium ions (Fig. 2B). Among the tested conditions, 1 M DEA and 1 mM $MgCl_2$ yielded the highest ALP activity. Thus, we then tested various pH conditions with 1 M DEA and 1 mM $MgCl_2$ (Fig. 2C). We found that pH 9.25 was the most optimal pH showing highest activity. Finally, we investigated the ALP activity at different 4-MUP concentrations to determine the basic kinetic parameters of ALP (Fig. 2D). By fitting the data points with the Michaelis-Menten equation, the maximum turnover rate (k_{cat}) and the Michaelis-Menten constant (K_M) were determined to be

1.19×10^3 s^{-1} and 183 μM, respectively. These values were consistent with a previous report on mutant ALP.[23]

Next, digital enzyme assays for detection of ALP activity in W/O-type femtoliter chambers were conducted at 2 mM 4-MUP in the presence of 1 M DEA and 1 mM $MgCl_2$ at pH 9.25, at which ALP hydrolyzes 4-MUP at 1090 s^{-1} according to the Michaelis-Menten analysis in Figure 2D. Note that the estimated consumption of 4-MUP in a 44 fL chamber containing single ALP molecule for 20 min reaction is only 2.5% so that the substrate consumption as well as product inhibition would be negligible. After adding the enzyme solution to the 4-MUP solution, the reaction mixture was immediately introduced into the device and sealed with fluorinated oil. When the calculated mean number of ALP molecules per chamber (λ) was well below 1, the chambers showed discrete fluorescent intensity. Figure 3A shows the fluorescence image at λ = 0.52 after a 4-min incubation. Although more than 50% of the chambers remained non-fluorescent, some chambers showed weak or strong fluorescence (Fig. 3B). The fractions of non-fluorescent, weak and strong fluorescent chambers were consistent with expectations based on the Poisson distribution. When ALP molecules are randomly encapsulated, the probability of encapsulation obeys the Poisson distribution:

$$P(k\ ;\lambda) = \frac{\lambda^k e^{-\lambda}}{k!}$$

where *P(k; λ)* represents the probability encapsulating *k* molecules. At λ = 0.52, the probabilities of having 0, 1, or 2 molecules per chamber were expected to be 59.5%, 30.9%, and 8.0%, respectively. The histogram of fluorescence intensities (Fig. 3A) showed clear discrete peaks for non-fluorescent chambers and chambers exhibiting weak fluorescence after fitting with a Gaussian. The chamber exhibiting strong fluorescence also appeared as a distribution on the rightmost of the histogram. The fractions of non-fluorescent, weakly, and strongly fluorescent chambers showed good agreement with the theoretical values for 0, 1, and 2 molecules (Fig. 3C). Excellent agreement between experimental and theoretical values was also confirmed at different λ (λ = 0.13, Fig. 3D). Thus, we concluded that the digital enzyme assay of ALP with the cumarin-based fluorogenic substrate 4-MUP has been achieved successfully.

Next, we conducted time-course analysis of digital enzyme assays of ALP at λ = 0.13. To minimize the photobleaching of 4-MU, images were taken at every 5 min with a 100-ms exposure time (Fig. 4A). The rate of increase in fluorescence intensity was determined for each chamber by linear fitting of the time course (Fig. 4B). Fig. 4C shows the distribution of the rate. The leftmost peak represents the non-fluorescent chamber (0 molecule). The second peak, magnified in the inset of Fig. 4B represents the catalytic activity of a single ALP molecule at 2 mM 4-MUP. The Gaussian fit yielded an average turnover rate of 891 s^{-1}. This value was slightly lower than the expected value

from the measurement shown in Fig. 2D (1090 s^{-1}). We do not attribute it to slow leakage of the fluorescent reaction product 4-MU into oil phase, because the chambers enclosed with 4-MU retained almost constant fluorescence over 30 min in control experiments (data not shown). Frequent interaction of enzyme with surfaces might interfere with the catalysis to some extent. As expected from the Poisson distribution with $\lambda = 0.13$, a few chambers (0.7%) showed double activity by encapsulation of two enzyme molecules in a chamber (Fig. 4A and 4B).

In order to determine the LOD of digital counting of ALP, a 10-fold dilution series of ALP solution from $\lambda = 0.13$ to $\lambda = 0.00013$ was subjected to digital enzyme assays. After a 10-min incubation, 120 fluorescence images of the different field of view were taken for each dilution sample. Figure 5A shows typical fluorescence images. Each field of view contains 7600 chambers, and the total number of chambers analyzed was over 0.9 million. Because the fraction of encapsulation of two enzyme molecules in a chamber was essentially negligible at $\lambda \leq 0.13$, each fluorescent chamber was counted as one enzyme molecule. The threshold level for fluorescent chambers was set as the mean background level plus 10 times the standard deviation (SD) of the background fluorescence. As shown in Figure 5B, the number of fluorescent chambers was proportional to the λ and essentially consistent with the theoretical values, although the experimental values were slightly higher than the theoretical values presumably due to the inaccuracy of protein quantification. The background count (false-positive fluorescent chambers detected in the absence of ALP) was much higher than that for the fluorogenic digital enzyme assay of β-gal with fluorescein-di-β-D-galactopyranoside (about 0.0001%).[19] This difference could be explained by contaminating impurities or photoresist remained on the device (see the Discussion). The high background count resulted in the LOD of 7.0 fM ($\lambda = 1.9 \times 10^{-4}$).

Finally, we tested the feasibility of dual-color digital enzyme assays of ALP and β-gal. In the fluorogenic assay for β-gal, the enzyme cleaved resorufin-β-D-galactopyranoside (RGP) to galactose and resorufin, yielding red fluorescence. The 4-MU and resorufin have different fluorescence emission peaks, 445 nm and 585 nm respectively, and spectrally separable in the fluorescence images. Because the optimal pH values for ALP and β-gal are different, the assays were conducted at near alkaline conditions (pH 8.25), at which ALP retains 67% of maximum activity. After mixing well-diluted enzyme solutions with fluorogenic substrates, the reaction mixture was introduced into a flow cell and observed under a fluorescence microscope. Figure 6 shows a pseudo-colored overlay image of 4-MU and resorufin. Green and red represent the fluorescence of 4-MU and resorufin, respectively. As expected, the green and red fluorescent chambers were distributed randomly, with some showing both green and red fluorescence (Fig. 6, yellow arrow), indicating the simultaneous

encapsulation of ALP and β-gal. Thus, the feasibility of dual-color digital enzyme assays with cumarin- and resorufin-based fluorogenic assays was successfully demonstrated.

Discussion

This study presented a cumarin-based fluorogenic assay can be applied as a digital enzyme assay. Because many cumarin-based fluorogenic assays have been developed for analysis and detection of enzymes, digital enzyme assays using cumarin-based probes are expected to have a variety of applications. In addition, the present study also demonstrated a dual-color digital enzyme assay using cumarin and resorufin for the first time.

Although fluorescein- and resorufin-based digital enzyme assays have been reported independently, dual-color digital enzyme assays using these two probes have not been achieved due to overlap of their excitation and fluorescence spectra. However, cumarin emits fluorescence signals of distinctively shorter wavelengths. In this study, we verified that dual-color digital enzyme assays for ALP and β-gal were feasible using resorufin and cumarin. Dual-color digital enzyme assays are expected to enable multiplex digital ELISA; while such multiplex digital ELISAs have been reported using differently colored plastic beads to identify captured antigen molecules,[21] the expansion of color variations in digital enzyme assays will provide an alternative approach for multiplex digital ELISA or further expand the multiplicity of digital ELISA by combination with the multi-colored bead method.

In addition to the above, multi-color digital enzyme assays are expected to exhibit improved background count compared with digital ELISA; high background count may impair the potential sensitivity of digital ELISA. The main factor affecting the background count in digital ELISA is non-specific binding of the detection antibody-enzyme conjugate to the bead surface on which the capture antibody is immobilized. Plastic beads are the most frequently used surface for antigen capture. When the target antigen molecule is marked with two different detection antibody-enzyme conjugates simultaneously, we can distinguish the true signal from the false-positive signal with high efficiency. This is because simultaneous non-specific binding of two detection conjugates on the same bead should be much more infrequent than single nonspecific binding events. Thus, by increasing the color variations of fluorogenic assays, the background count of digital ELISAs will be dramatically reduced. This strategy is expected to be highly effective, particularly for digital ELISAs targeting multi-epitope antigens such as infectious viruses.

However, several drawbacks of this method were also found when compared with fluorescein-based digital enzyme assay. The first one is leakage of cumarin to the fluorinated oil

phase under neutral pH conditions. Although 4-MU has an additional hydroxyl moiety on the cumarin structure which enhances water solubility, the hydroxyl group of 4-MU has to be deprotonated to prevent the leakage into the fluorinated oil phase. Actually, slow leakage was found at neutral pH (pH 7.0). This phenomenon is consistent with the pK_a of the hydroxyl group of 4-MU (pH 7.8). Thus, 4-MU-based fluorogenic assays are currently limited to the conditions in which the pH is alkaline or near alkaline. Several cumarin derivatives carrying dissociative groups with different pK_a values have been reported. To expand the cumarin-based fluorogenic assay to the conditions in which the pH is neutral or acidic, cumarin derivatives with lower pK_a, such as fluorinated 4-MU, should be tested.

Another drawback of cumarin-based digital enzyme assays is their relatively high background count. As shown in Figure 5B, 0.03–0.04% of chambers showed apparent fluorescence signals under ALP-free conditions. Thus, because of this high background count, the digital counting of ALP with 4-MUP has not achieved the LOD below the fM level. We tested possible contamination of ALP enzymes from bacteria grown in buffers by using freshly prepared chemicals and buffers. However, the background count was not reduced. However, when observed with an optical setup for fluorescein imaging, such background counts were not observed. The background count was observed even when pure water was introduced in the device. These results suggest that the background count was attributable to dissolution of unknown impurities from CYTOP or photoresist polymers. Thus, to reduce or eliminate the background count, microfabrication procedures may have to be improved.

Experimental

Materials

The D101S mutant of alkali phosphatase (ALP) from *E. coli* was a kind gift from Abott Japan.[23] Powder of ALP was dissolved in buffer A (20 mM Tris-HCl, pH 8.0, 1 mM $MgCl_2$, 150 mM NaCl, 0.1% sodium azide) and stored at -30°C. The ALP stock was diluted in buffer A before use. Enzymatic activity was measured in assay buffer containing the indicated concentrations of diethanolamine (DEA)-HCl at pH 9.25 and magnesium chloride. The fluorogenic substrate for ALP, 4-methylunbelliferyl phosphate (4-MUP) and the reaction product, 4-metylunbelliferon (4-MU) were purchased from Sigma Aldrich (St. Louis, MO, USA). Stock solutions of 4-MUP and 4-MU were dissolved in dimethyl sulfoxide (DMSO) and stored at -30°C.

ALP assay in bulk solution

ALP activity in bulk solution was measured in 96-well black plates (Greiner, Germany). Stocks of 4-MUP and ALP solutions were diluted in 200 μL assay buffer. The time course of fluorescence intensity (excitation: 372 nm, emission: 445 nm) was measured at 28°C with 30 s intervals for 5 min with a microplate reader (Flex Station 3; Molecular Devices, USA). The turnover rate was estimated from the linear fitting of the time-course and the calibration curve between fluorescence intensity and 4-MU concentration.

Microfabrication of the femtoliter chamber array

Chamber array devices were prepared as previously reported.[19] A glass coverslip (24 × 32 mm) was sonicated in acetone, isopropanol, and deionized water for 10 min each. After sonication treatment, the coverslips were immersed in 10 M KOH for several hours and rinsed with deionized water. The coverslips were then spin-coated with amorphous fluorocarbon polymer (CYTOP 816AP; Asahi Glass, Japan) at 3000 rpm for 30 s and baked for 1 h on a hotplate at 180°C. The thickness of the CYTOP layer was 3 μm. The CYTOP-coated coverslip was spin-coated with a positive photoresist (AZ-4903; AZ Electronic Materials, USA) at 4000 rpm for 60 s and baked at 55°C for 3 min and then 110°C for 5 min. Subsequently, photolithography was carried out with a mask structure with 3 μm holes, which were each separated by 3 μm. The resist-patterned coverslip was dry-etched with O_2 plasma in a reactive ion etching system (RIE-10NR; Samco, Japan) to remove exposed CYTOP. The substrate was then cleaned and rinsed with acetone and ethanol to remove the photoresist layer remaining on the substrate. The resulting CYTOP-on-coverslip devices had an array of exposed SiO_2 patterns with diameter of 4.3 μm, which each held a water droplet in the digital enzyme assay. The device had 120 square areas each having 28223 (167 × 169) patterns within an area of 10 × 10 mm^2.

Digital enzyme assay for ALP in the chamber array

The flow cell was constructed from a CYTOP-on-coverslip device and a non-fabricated coverslip, which were bound via a paper spacer with silicone grease. The ALP stock solution was diluted with assay buffer containing 1.1 mg/mL Tween20 (Sigma Aldrich) and 2 mM 4-MUP. Next, 40 μL of reaction mixture was introduced in the flow cell by manual pipetting. Then, 200 μL of fluorinated oil (Fluorinert FC-40; Sigma) was introduced into the flow cell to flush out an excess amount of reaction mixture and form W/O droplets on the 4.3 μm wells of the device. The enzymatic activity of ALP molecules in chambers was measured from the fluorescence signal of the catalytically produced 4-MU under a fluorescence microscope.

Fluorescence image analysis

Fluorescent images were observed with a CMOS camera (Neo sCMOS camera; Andor, UK) on an inverted microscope (IX81; OLYMPUS, Japan) equipped with a 20× objective lens (UPlanSApo 20×/0.75; OLYMPUS) and a 1.6× image extender lens (in total 32× image magnification). The 120 fluorescence images of the different field of view (each contains 7600 chambers) in a device were taken with 100-ms exposure time for each, and analyzed with image analysis software (MetaMorph; Molecular Devices). The fluorescence intensity of each chamber was determined as the averaged intensity of 7 × 7 pixels (1.4× 1.4 μm^2) containing a single chamber.

Dual digital enzyme assay

The indicated amount of ALP and β-gal from *E. coli* (Roche Applied Science, USA) was mixed in buffer B (1 M diethanolamine-HCl, pH 8.25, 1 M $MgCl_2$) containing 250 μM 4-MUP and 250 μM resorufin-β-D-galactopyranoside (RGP) (Lifetechnologies, USA). After infusion into the flow cell and sealing with FC 40 oil, the chambers were imaged with a confocal microscope (Nikon Eclipse Ti microscope; Nikon, Japan) equipped with a CMOS camera (NIKON A1R MP; Nikon). The objective lens used was PlanApo 60×/1.40 oil (Nikon), and 401 nm and 561 nm lasers were used as the excitation light sources for 4-MU and resorufin, respectively.

Acknowledgements

We would like to thank Dr. Toru Yoshimura, Dr. Eisaku Yoshida, and Dr. Ryotaro Chiba from Abbott Japan for the expression vector of the mutant ALP and for technical supports. This research was supported by Japan Science and Technology Agency for Core Research for Evolutional Science and Technology (CREST).

References

1. Schneider, T., Kreutz, J., and Chiu, D. T. (2013) The potential impact of droplet microfluidics in biology. *Analytical chemistry* **85**, 3476-3482
2. Witters, D., Sun, B., Begolo, S., Rodriguez-Manzano, J., Robles, W., and Ismagilov, R. F. (2014) Digital biology and chemistry. *Lab on a chip* **14**, 3225-3232
3. Ge, S., Liu, W., Schlappi, T., and Ismagilov, R. F. (2014) Digital, ultrasensitive, end-point protein measurements with large dynamic range via Brownian trapping with drift. *Journal of the American Chemical Society* **136**, 14662-14665
4. Liebherr, R. B., Renner, M., and Gorris, H. H. (2014) A single molecule perspective on the functional diversity of in vitro evolved beta-glucuronidase. *Journal of the American Chemical Society* **136**, 5949-5955
5. Rissin, D. M., Gorris, H. H., and Walt, D. R. (2008) Distinct and long-lived activity states of single enzyme molecules. *Journal of the American Chemical Society* **130**, 5349-5353
6. Rondelez, Y., Tresset, G., Tabata, K. V., Arata, H., Fujita, H., Takeuchi, S., and Noji, H. (2005) Microfabricated arrays of femtoliter chambers allow single molecule enzymology. *Nature biotechnology* **23**, 361-365
7. Bar-Even, A., Noor, E., Savir, Y., Liebermeister, W., Davidi, D., Tawfik, D. S., and Milo, R. (2011) The moderately efficient enzyme: evolutionary and physicochemical trends shaping enzyme parameters. *Biochemistry* **50**, 4402-4410
8. Rotman, B. (1961) Measurement of activity of single molecules of beta-D-galactosidase. *Proceedings of the National Academy of Sciences of the United States of America* **47**, 1981-1991
9. Rissin, D. M., and Walt, D. R. (2006) Digital concentration readout of single enzyme molecules using femtoliter arrays and Poisson statistics. *Nano letters* **6**, 520-523
10. Sakakihara, S., Araki, S., Iino, R., and Noji, H. (2010) A single-molecule enzymatic assay in a directly accessible femtoliter droplet array. *Lab on a chip* **10**, 3355-3362
11. Shim, J. U., Ranasinghe, R. T., Smith, C. A., Ibrahim, S. M., Hollfelder, F., Huck, W. T., Klenerman, D., and Abell, C. (2013) Ultrarapid generation of femtoliter microfluidic droplets for single-molecule-counting immunoassays. *ACS nano* **7**, 5955-5964
12. Watanabe, R., Soga, N., Fujita, D., Tabata, K. V., Yamauchi, L., Hyeon Kim, S., Asanuma, D., Kamiya, M., Urano, Y., Suga, H., and Noji, H. (2014) Arrayed lipid bilayer chambers allow single-molecule analysis of membrane transporter activity. *Nature communications* **5**, 4519
13. Rondelez, Y., Tresset, G., Nakashima, T., Kato-Yamada, Y., Fujita, H., Takeuchi, S., and Noji, H. (2005) Highly coupled ATP synthesis by F1-ATPase single molecules. *Nature* **433**, 773-777
14. Cai, L., Friedman, N., and Xie, X. S. (2006) Stochastic protein expression in individual cells at the single molecule level. *Nature* **440**, 358-362
15. Sims, P. A., Greenleaf, W. J., Duan, H., and Xie, X. S. (2011) Fluorogenic DNA sequencing in PDMS microreactors. *Nature methods* **8**, 575-580

16. Iino, R., Hayama, K., Amezawa, H., Sakakihara, S., Kim, S. H., Matsumono, Y., Nishino, K., Yamaguchi, A., and Noji, H. (2012) A single-cell drug efflux assay in bacteria by using a directly accessible femtoliter droplet array. *Lab on a chip* **12**, 3923-3929

17. Kim, S. H., Yoshizawa, S., Takeuchi, S., Fujii, T., and Fourmy, D. (2013) Ultra-high density protein spots achieved by on chip digitalized protein synthesis. *The Analyst* **138**, 4663-4669

18. Ehrl, B. N., Liebherr, R. B., and Gorris, H. H. (2013) Single molecule kinetics of horseradish peroxidase exposed in large arrays of femtoliter-sized fused silica chambers. *The Analyst* **138**, 4260-4265

19. Kim, S. H., Iwai, S., Araki, S., Sakakihara, S., Iino, R., and Noji, H. (2012) Large-scale femtoliter droplet array for digital counting of single biomolecules. *Lab on a chip* **12**, 4986-4991

20. Rissin, D. M., Kan, C. W., Campbell, T. G., Howes, S. C., Fournier, D. R., Song, L., Piech, T., Patel, P. P., Chang, L., Rivnak, A. J., Ferrell, E. P., Randall, J. D., Provuncher, G. K., Walt, D. R., and Duffy, D. C. (2010) Single-molecule enzyme-linked immunosorbent assay detects serum proteins at subfemtomolar concentrations. *Nature biotechnology* **28**, 595-599

21. Rissin, D. M., Kan, C. W., Song, L., Rivnak, A. J., Fishburn, M. W., Shao, Q., Piech, T., Ferrell, E. P., Meyer, R. E., Campbell, T. G., Fournier, D. R., and Duffy, D. C. (2013) Multiplexed single molecule immunoassays. *Lab on a chip* **13**, 2902-2911

22. Gorris, H. H., Rissin, D. M., and Walt, D. R. (2007) Stochastic inhibitor release and binding from single-enzyme molecules. *Proceedings of the National Academy of Sciences of the United States of America* **104**, 17680-17685

23. Mandecki, W., Shallcross, M. A., Sowadski, J., and Tomazic-Allen, S. (1991) Mutagenesis of conserved residues within the active site of Escherichia coli alkaline phosphatase yields enzymes with increased kcat. *Protein engineering* **4**, 801-804

24. McComb, R. B., and Bowers, G. N., Jr. (1972) Study of optimum buffer conditions for measuring alkaline phosphatase activity in human serum. *Clinical chemistry* **18**, 97-104

Figure Legends

Figure 1. Fluorogenic substrate and enzyme used in this study

Schematic image of the fluorogenic assay of alkaline phosphatase (ALP) which hydrolyzes 4-methylunbelliferyl phosphate (4-MUP) to 4-metylunbelliferon (4-MU) and inorganic phosphate. While 4-MUP is non-fluorescent, 4-MU is fluorescent (excitation peak: 372 nm, emission peak: 445 nm).

Figure 2. Fluorogenic assay of ALP in bulk solution

(A) Time courses of fluorogenic assays of ALP with 4-MUP at 300 μM (red), 1 mM (green), 3 mM (blue). The reaction was monitored by the fluorescence of the reaction product, 4-MU. The turnover rate was determined from the linear fitting of a time-course. (B) Effects of diethanolamine (DEA) and magnesium chloride on the turnover rate. (C) pH dependence of the turnover rate. The activity was measured in the presence of 1 M DEA and 1 mM $MgCl_2$. Error bars represent standard deviations of three independent measurements. (D) Dependence of turnover rate on 4-MUP concentration. The activity was measured in the presence of 1 M DEA and 1 mM $MgCl_2$ at pH 9.25. Data points were fitted to the Michaelis-Menten equation to give a K_m of 183 μM and a V_{max} of 1.19×10^3 s^{-1}.

Figure 3. Digital enzyme assay of ALP

(A) Fluorescence images of digital enzyme assays of ALP with a 44-fL chamber array device at the mean number of ALP molecules per chamber (λ) of 0.52. Images were taken after a 10-min incubation. The exposure time was 100 ms. (B) Distribution of the fluorescence intensity of the chambers. The data points were fit to the sum of the three Gaussians. Chambers were assigned to having 0, 1, or 2 enzymes according to the fluorescence intensity. (C) The fractions of chambers with 0, 1, and 2 enzymes experimentally determined by the Gaussian fitting in (B) (blue), and the theoretical value estimated assuming the Poisson distribution with $\lambda = 0.52$. (D) The fractions of chambers with 0, 1, or 2 enzymes when $\lambda = 0.13$.

Figure 4. Time-course analysis of the digital enzyme assay of ALP

(A) Fluorescence images after 5, 10, 15, and 20 min. $\lambda = 0.13$. (B) Time course of the fluorescence intensity from (A). Orange, green, and light blue lines were assigned to chambers with 0, 1, and 2 enzymes, respectively. (C) Distribution of the rate of fluorescence increase determined by linear fitting of (B). The data points were fit to the sum of two Gaussians for chambers having 0 (orange) or

1 (green) enzyme molecule. Blue data points were assigned to chamber having 2 enzyme molecules. Inset indicates enlarged distribution of chambers having 1 or 2 enzymes.

Figure 5. Digital counting of ALP

(A) Fluorescence images of digital enzyme assays of ALP at λ = 0.13, 0.013, 0.0013, and 0.00013 after a 10-min incubation. Typical examples of single field of view obtained at each λ are shown. The numbers of fluorescent chambers (n) at each λ is also shown. (B and C) The fraction of fluorescent chambers versus λ (B) or ALP concentration (C). Error bars are standard deviations of three independent measurements. The red line represents the fraction of background count plus 3 times the SD of the background count determined in the ALP-free condition.

Figure 6. Dual-color digital enzyme assay for ALP and β-gal

Dual-color fluorogenic assays for ALP and β-gal were conducted by a 45-min incubation. ALP and β-gal were encapsulated at λ=0.033 and 0.05, respectively. ALP produced 4-MU, and β-gal produced resorufin. A pseudo-colored overlay image of 4-MU (green) and resorufin (red) was shown. The yellow color indicates a mixture of red and green signals, representing the coexistence of ALP and β-gal.

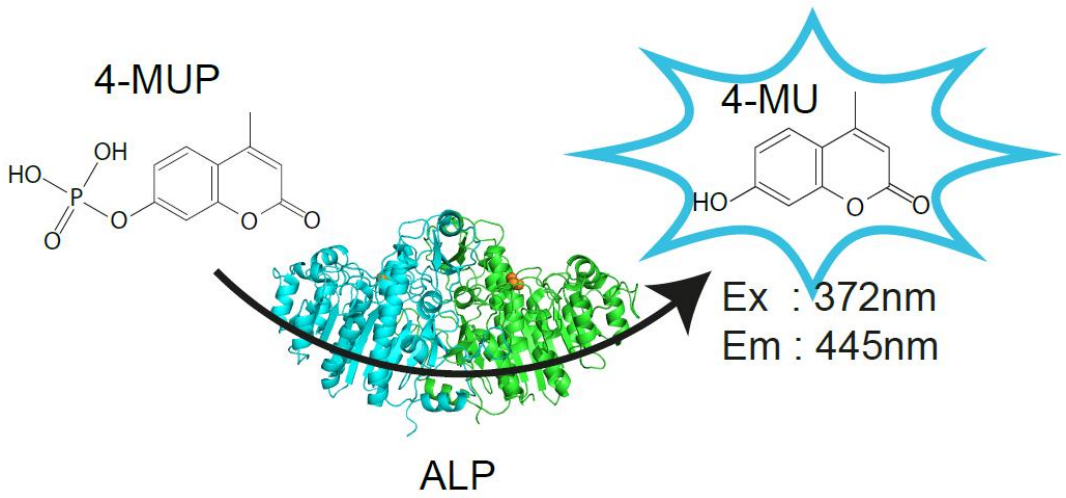

Obayashi Figure 1